Volume 150
Number 5
7 March 2025
Pages 797-1024

Analyst

rsc.li/analyst

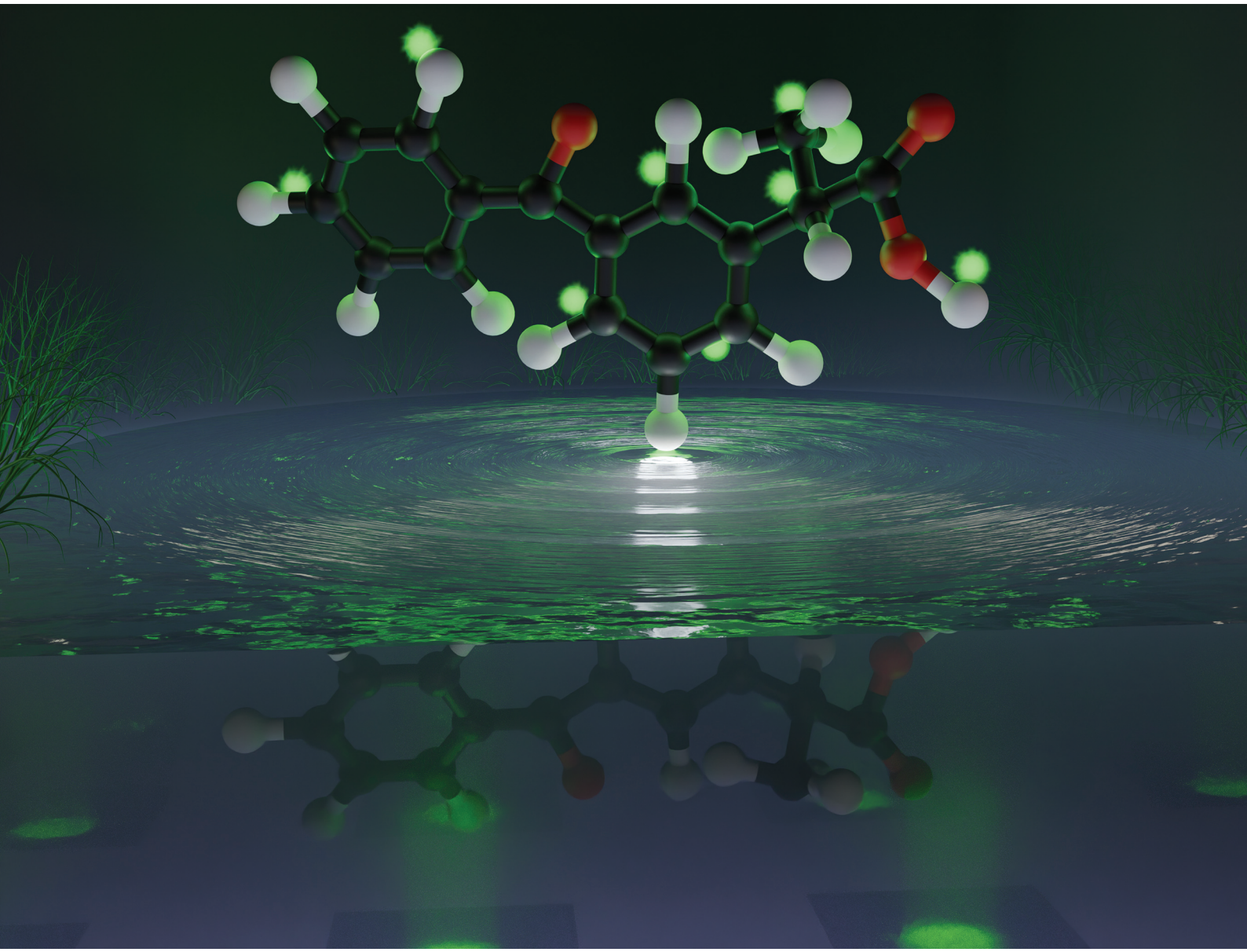

ISSN 0003-2654

ROYAL SOCIETY OF CHEMISTRY

PAPER

Giammarco Maria Romano, Larisa Lvova *et al.*
A bis-pyrene polyamine receptor for fast optical detection of ketoprofen: synthesis, characterization and application in all-solid-state fluorescent sensors

150 YEARS ANNIVERSARY

Analyst

ROYAL SOCIETY OF CHEMISTRY

PAPER

View Article Online
View Journal | View Issue

Cite this: *Analyst*, 2025, **150**, 806

A bis-pyrene polyamine receptor for fast optical detection of ketoprofen: synthesis, characterization and application in all-solid-state fluorescent sensors†

Giammarco Maria Romano, *[a] Pierangela Di Menna,[b] Andrea Bencini, [a] Yschtar Tecla Simonini Steiner, [a] Massimo Innocenti, [a] Corrado Di Natale, [c] Roberto Paolesse [b] and Larisa Lvova *[b]

Herein, we report on a polyamine receptor L1 bearing pyrene fluorogenic groups for the optical assessment of the non-opioid analgesic drug ketoprofen (KP). L1, composed of a diethylenetriamine moiety linked at its extremities to the 1 position of two pyrene units *via* methylene linkers, produced an emission at 460 nm in 1 : 1 (v/v) water/ethanol mixture at pH 7, which can be attributed to the excimer formation between the two aromatic groups. In the presence of KP, a salt-bridging interaction between the carboxylate group of the analyte and the central ammonium group of L1 induced a redistribution of acidic protons in the polyamine chain, causing a marked increase in the emission. This optical signal was used to detect KP in aqueous media. Based on this observation, the properties of all-solid-state optodes with plasticized PVC membranes doped with L1 and deposited on an appropriate solid support material were further investigated. The best membrane contained 1 wt% of fully protonated L1, plasticized with DOS and doped with 3 equiv. of the TDMACl anion-exchanger, which detected KP in the 2 μM–0.1 mM range with a low influence of interfering ions. Furthermore, this membrane was applied for the assessment of the amount of KP in OkiTask, achieving an RSD of 2.1% and recovery of 102%. Moreover, the possibility to decrease the LOD of KP to 0.84 μM (0.21 mg L^{-1}) through the application of L1-based fluorescent sensor arrays and chemometrics was studied.

Received 25th November 2024,
Accepted 19th January 2025

DOI: 10.1039/d4an01469c

rsc.li/analyst

1. Introduction

Among the non-steroidal anti-inflammatory drugs (NSAIDs), ketoprofen (KP) is one of the most widely used to reduce various types of inflammations, muscle pain and headache; to lower fever as well as counter cold and flu symptoms.[1] The main mechanism of action of KP is *via* the inhibition of prostaglandin synthesis with the cyclooxygenase enzyme, making it effective against acute and chronic pain in arthrosis and arthritis. In medicine, either its acidic form (KPH) or more soluble salt form (ketoprofen lysine salt, KP-Lys) is the main component of many pharmacological compositions for oral submission for adults and children and in skin-treatment pastes and gels, wound treat dressings, *etc.*[2,3]

Although KP is a readily degradable compound characterized by low environmental stability, its inflow to ground and surface waters is constant owing to its excessive use and production.[4,5] Existing wastewater treatment plants (WWTPs) are not specifically designed to eliminate NSAIDs, allowing only partial reduction of their concentration. Thus, more hydrophilic drugs may pass through treatment processes, resulting in significant environmental concentrations and exposure to living organisms.[6] Besides, several side-effects, such as poor tolerance of the gastrointestinal tract, allergy induction, liver and kidney dysfunctions, and light sensitization, can result upon high dose consumption or long-term medication. Several studies have proved that KP toxicity is potentially associated with many chronic medical conditions such as cardiovascular diseases, renal failure and endocrine disruption.[7] KP has recently been acknowledged as an emerging contaminant with considerable environmental implications, attributable to its long-term toxic effects, absence of effective removal methods from waste, and marked increase in consumption during the COVID-19 pandemic and the subsequent period.[8,9]

[a]*Department of Chemistry "Ugo Schiff", University of Florence, Via della Lastruccia 3, 50019 Sesto Fiorentino, Italy. E-mail: giammarcomaria.romano@unifi.it*
[b]*Department of Chemical Sciences and Technologies, University "Tor Vergata", Via della Ricerca Scientifica 1, 00133 Rome, Italy. E-mail: larisa.lvova@uniroma2.it*
[c]*Department of Electronic Engineering, University "Tor Vergata", Via del Politecnico 1, 00133 Roma, Italy*

† Electronic supplementary information (ESI) available. See DOI: https://doi.org/10.1039/d4an01469c

The detection of anti-inflammatory KP drug in pharmaceutical compositions and environmental samples is an important analytical task, and several analytical techniques have been previously reported for the assessment of NSAIDs, in particular KP, including chromatography,[10] spectrophotometry,[11,12] electrochemical,[13–15] optical sensors,[16–20] and multisensory arrays.[21,22] Among different transduction-type sensors, optical sensors have the advantages of fast response time, simplicity of preparation and signal acquisition, as well as the possibility to achieve low detection limits and high sensitivity.[23–28] Moreover, these devices do not require sophisticated hardware, are wireless and their output may be estimated with common optoelectronic devices or even through visual observation in a "naked-eye" mode.[29–31] In the last few years, several nanostructured assemblies have been used for the optical signaling of KP, among them are differently modified quantum dots (QDs),[16,17] metallic nanoparticles,[18] and composite materials such as molecularly imprinted polymers (MIPs),[19] hydrogels,[20] or specific polymer-based sensors arrays.[22] Delgado-Pérez *et al.* developed CdSe/ZnS quantum dots bearing a chiral organic ligand for the enantioselective recognition of KP; however, no selective recognition among the NSAIDs KP, flurbiprofen, and naproxen was achieved.[17] Bhogal *et al.* reported a hybrid fluorescent material composed of carbon dots–molecularly imprinted polymer (CDs–MIPs), which was selectively quenched by KP in a water solution, with applications in the determination of KP in human serum and urine samples.[19] A simultaneous detection system in a water/ethanol mixture for naproxen and ketoprofen was also proposed by Wang *et al.* exploiting two different FMIPs. The system showed high specificity towards each NSAID and LODs at the nanomolar level.[32]

Significantly less focus has been directed towards fluorescent small molecules for the detection of ketoprofen. Examples of supramolecular arrays exploiting hydrogen-bonding chemosensors, such as calix[4]pyrroles as receptor units,[33] BINOL derivatives for the enantiomeric recognition of NSAIDs,[34] and calixpyrrole-type macrocycles for KP sensing,[35] have been previously explored. In this regard, polyamine receptors bearing aromatic signaling units[36] are potentially appealing receptors for NSAIDs as they present common structural features, being normally composed of a carboxylic group, which are usually deprotonated at neutral pH, linked to an aromatic portion. Polyamines can protonate in aqueous solution even at pH 7, and the resulting polyammonium cations can give H-bonding and charge–charge contacts between NSAID carboxylate groups. In polyamine-based fluorescent receptors, this interaction is expected to result in an overall fluorescence intensity emission change, which may be correlated to the pain-killer compound concentration in the analyzed sample.[37,38] A recent work by Romano *et al.* reported on open-chain polyamine receptors equipped with two anthracene fluorogenic fragments at their extremities for KP sensing in water/ethanol solutions upon excitation at 340 nm.[36] However, chemosensor response to KP was registered in quite a narrow concentration range from 0 to 5.0 equiv. with respect to the ligand. ^{1}H NMR titrations demonstrated no direct involvement of the aromatic anthracene units in KP binding *via* π-stacking interactions, which may be the reason for such a small KP concentration working range.

To increase the linear working range, the introduction of fluorescent signaling units other than anthracene on polyamine scaffolds can be useful. To this purpose, we linked two pyrene units at the terminal amine groups of a diethylenetriamine chain to explore the ability of the two large aromatic moieties to stack together and give excimer emission in aqueous solution, which can be modulated upon substrate coordination. In the present study, we investigated the properties of this receptor for selective and rapid assessment of KP in aqueous media. Since the construction of all-solid-state optical sensors is more practical and easier to handle in comparison to the common optical sensing methodology when an analyte is added to the solution containing an optically active receptor, we have focused on the development of all-solid-state fluorescent sensors for KP detection. To this purpose, we tested PVC polymeric membranes containing either the three-hydrochloride form of the receptor, L1·3HCl, and its unprotonated form, L1 (Scheme 1), for KP sensing. Our purpose was the improvement of sensor analytical characteristics through the accurate tuning of sensing membrane composition to select an appropriate solid support material, together with the interpretation of the signal transduction mechanism. Moreover, a multisensory approach was employed to lower the KP detection limit of the developed optodes.

2. Experimental section

2.1 Reagents and L1·3HCl, L1 syntheses

The detailed list of reagents used is provided in section S1 of ESI,† while the synthetic details for L1 and its hydrochloride salt are reported in section S2.† L1 was synthesized, as sum-

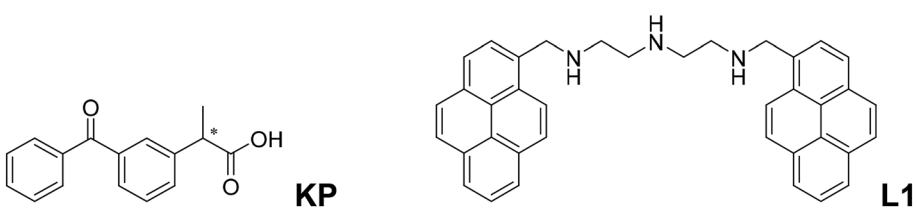

Scheme 1 Structures of KP and the L1 receptor.

marized in Scheme S1,† using a slightly modified procedure commonly used for the terminal alkylation of linear polyamines.[39,40] The characterization data for L1·3HCl and L1 are given in Fig. S2–S6.†

2.2 Electronic absorption and fluorescence measurements

Absorption spectra were recorded on a Jasco V-670 spectrophotometer using ligand concentrations of 5×10^{-7} M. Emission spectra were recorded on a Horiba Scientific Fluoromax Plus fluorimeter using an excitation wavelength of 360 nm and ligand concentrations of 5×10^{-7} M. All measurements were performed in a water/ethanol 1 : 1 (v/v) mixture at pH 7 using a 0.005 M Tris/HCl buffer at 298.0 ± 0.1 K. Measurements at different pH values were performed in a 1 : water/ethanol 1 (v/v) mixture with 0.1 M NMe_4Cl to maintain the ionic strength (pK_w = 14.52(1) in the above stated condition).[41] The binding tests were performed by spectrophotometric and spectrofluorimetric titrations at the pH of an L1 solution in the presence of increasing amounts of different analytes. Luminescence quantum yields were determined using quinine sulfate in a 0.05 M H_2SO_4 aqueous solution (Φ = 0.53) as a standard reference.[42]

2.3 NMR Measurements

NMR spectra were recorded on a Bruker 400 MHz (Bruker Corp., Billerica, MA, USA) instrument. NMR titrations were carried out in a D_2O/CD_3OD 40 : 60 (v/v) mixture at pH 7 by the addition of KP to 0.001 M solutions of L1. The pH was adjusted to 7 by adding small amounts of NaOD or DCl after each addition of KP to the solutions of L1.

2.4 Membranes preparation and sensing materials testing

Polymeric membranes were prepared by the incorporation of approximately 1 wt% of L1·3HCl or L1 and 1–3 equiv. of anion-exchanger (TDACl or TDMACl) into a polymeric matrix containing PVC and plasticizer (TOP or DOS) in 1 : 2 ratio by weight. The overall membrane weight was 100 mg; all the membrane components were dissolved in 1 mL of THF. Planar optodes were prepared through drop-casting method, for which a series of sensing spots was produced by deposition of 2 μL of each membrane cocktail on different solid supports: Whatman 1003–110 (390 mm, 185 g m^{-2}) filter paper (FP), color catcher cellulose tissue (CC), and glass slides (GS). After THF evaporation, optodes were tested for the optical assessment of primary KP and KP-Lys and interfering ions in 2×10^{-6}–1×10^{-4} M concentration range upon illumination with UV light at 365 nm and direct spiking of 5 μL of calibration solutions of different concentration every time on the new sensing spot.

All the solutions for optodes testing were prepared with distilled water at 0.005 M Tris/HCl background, pH 7.00. The pH was adjusted by adding small aliquots of 1 M HCl and simultaneously controlled with an AMEL pH-meter (Italy), preliminarily calibrated with pH 7.00 and pH 10.00 standard buffer solutions (Sigma-Aldrich, Germany).

2.5 Optical signal acquisition and data processing

For the quantification of optical response and its correlation to the KP content in the calibration and test solutions, optode images were acquired with a smartphone from a fixed distance of 10 cm upon excitation at 365 nm (see section S3 of ESI† for details). The whole sensing spot surface was considered as a region of interest (ROI); ROI luminescence intensity variations were then transformed into analytically useful digital signals by application of Colorpicker (**https://imagecolorpicker.com/**) and ImageJ (**https://ij.imjoy.io/**) freeware. Optode luminescent response was converted into three main colors of the visible spectrum–red (630 nm), green (530 nm), and blue (480 nm)–according to the RGB scale. The RGB values were extracted for each pixel of ROI, the color components were averaged, and these mean values were used for data analysis after subtraction of background without analyte and background without sensing spot. Measurements were performed for 3 solid supports and repeated twice for 3 consecutive measurement days (n = 6).

Standard addition method was used to estimate the KP amount in OkiTask by Dompé pharmaceutical composition. Details on sample preparation and analytical procedure are reported in section S4 of ESI.†

The data obtained from fluorescent multisensor array were treated with Unscrambler (CAMO PROCESS AS, Norway). PLS1 regression model was used to fit multisensor array optical response with KP concentrations in the calibration solutions; leave-one-out validation was applied due to the restricted number of measurements composing the dataset. RMSEC, RMSEV (Root Mean Square Error of Calibration and Validation respectively) and correlation coefficient, R^2, of predicted *vs.* measured correlation lines were used to evaluate the efficiency of the constructed regression models. The low detection limit of KP detection was estimated by 3σ method (LOD = $3\sigma/S$, where σ is the RMSEC recalculated in mg L^{-1} and S is the slope of the regression line at calibration stage) (for details on LOD calculations, see section S5 of ESI†).

3. Results and discussion

3.1 Acid–base properties of L1

The determination of protonation characteristics of a polyamine-based fluorescent host is the preliminary step to analyze the effect of pH on its emission properties and binding/detection ability for anionic substrates. To this purpose, UV-Vis and fluorescence emission spectroscopy were used to study the photophysical characteristics of the present receptor at different pH values. Measurements were performed in a H_2O/EtOH 1 : 1 (v/v) mixture to ensure the complete solubility of the ligand in a wide pH range (3–11.5). The absorption spectrum of L1 shows the classic pyrene absorption band with a maximum at 345 nm and a red-shifted tail (*ca.* 360 nm), which increases with increasing pH (Fig. 1a). This suggests the formation of an intramolecular ground-state dimer (GSD) between the two pyrene units, which is more favored at alka-

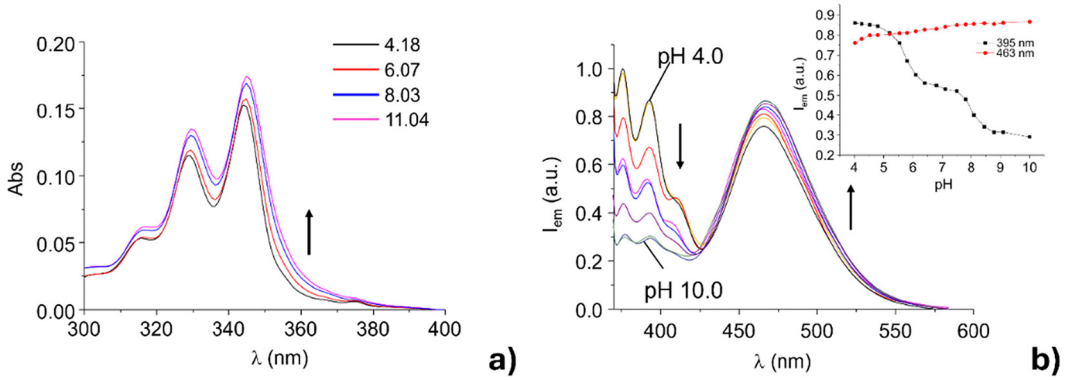

Fig. 1 Absorption spectra (a) and selected fluorescence emission spectra (b) of L1 at different pH values in H_2O : EtOH (1 : 1 v/v) mixture and 0.1 M NMe_4Cl. Inset of (b) shows a plot of the fluorescence emission intensity at 395 nm and 463 nm ([L1] = 1×10^{-6} M, λ_{exc} = 360 nm).

line pH values.[43] In fact, the triamine chain is likely to be protonated at acidic pH values. Its progressive deprotonation with increasing pH enhances its flexibility and allows the whole receptor to assume a conformation in which the two pyrene units are close to one another, favoring their interaction *via* hydrophobic and/or π-stacking. Direct photoexcitation of this GSD at 360 nm gives rise to a broad emission band centered at 463 nm typical of the excimer form of pyrene.[44–46] As shown in Fig. 1b, at slightly acidic, neutral, and alkaline conditions, L1 exhibits both a typical structured emission band at 370–430 nm (λ_{exc} = 360 nm) corresponding to monomer emission, and a second red-shifted band at 460 nm, attributed to the formation of intramolecular excimer species. The progressive deprotonation of the ammonium groups with increasing pH results in a decrease in intensity of the monomer emission at 395 nm and, to a lesser extent, in an increase of the excimer emission at 460 nm. Most likely, deprotonation of the triamine chain induces an increase in the electron density at the nitrogen atoms, favoring a photo-induced electron transfer (PET) effect from an amine group to the excited fluorophore that leads to quenching of the monomer emission at 395 nm and justifies the slight increase in dimer emission at 460 nm. The emission intensity at 395 nm remains almost constant between pH 4 and 5 (Fig. 1a, inset). At higher pH values, the emission decreases again to achieve a constant value in the pH range of 6.5–7.5. Above pH 7.5, the emission increases again and finally assumes a nearly constant value above pH 9. Treatment of the emission intensity data at 395 nm using the HypSpec program[47] allows for the calculation of protonation constants of 8.1(1) and 5.9(1) log units, corresponding to the formation of a mono- and di-protonated receptor L1, respectively.

These values are very similar to those found for the corresponding bis-anthracenyl derivative of 1,4,7-diethylenetriamine,[36] for which a third protonation step was also observed at acidic pH values (pK_a = 3.3), as normally found in diethylenetriamine and its derivatives.[48] In the present case, precipitation in H_2O/EtOH below pH 3.5 prevents spectrum collection and determination of the constant relative to the third protonation step of the receptor. The calculated constants for the first and second protonation equilibrium allow to conclude that the receptor is mainly in its mono-protonated form at neutral pH. Considering that benzylic amine groups adjacent to aromatic moieties are normally less basic,[49] we can reasonably conclude that in the monoprotonated species, the acidic proton is localized on the central amine groups of the triamine chain at a larger distance from the pyrene units.

3.2 Binding properties of L1 toward KP in water/ethanol solution

3.2.1 UV-Visible and fluorescence measurements. To investigate the binding abilities of bis-pyrene-substituted triamine receptor toward KP and its optical response, we performed UV-vis and fluorescence emission titrations by adding increasing amounts of the KP analyte to a 0.5 μM solution of L1 in H_2O/EtOH mixture (1 : 1 v/v) buffered at pH 7 with Tris. Preliminary tests did not demonstrate evident changes in the UV-vis spectra upon increase in the KP concentration, suggesting that no L1 structural changes occur upon binding with KP in the ground state (Fig. S7†). On the contrary, a significant increase of the emission band of the excimer species, centered at *ca.* 460 nm, was recorded upon excitation of L1 at 360 nm upon the addition of KP (Fig. 2).

The intensity of the monomer band at about 375–400 nm remains almost constant. Notably, the emission of the 460 nm band increases almost linearly up to a 1.8 : 1 KP : L1 molar ratio (R). At higher R values, the emission achieves an almost constant value for molar ratio greater than 2.5, with a quantum yield Φ of 0.37 (Φ = 0.25 for L1 in the absence of KP). This suggests the formation of adducts with both 1 : 1 and 1 : 2 receptor to substrate stoichiometry. Indeed, the analysis of the spectrofluorimetric data with HypSpec program[48] shows the formation of complexes with receptor to substrate stoichiometry of 1 : 1 and 1 : 2 with estimated apparent binding constants at pH 7.0 (ligand speciation not analytically considered) for the successive addition of one ($HL1^+ + KP^- = [HL1(KP)]$) and two ($[HL1(KP)] + KP^- = [HL1(KP)_2]^-$) KP anions to L1 of 4.1 (1) and 3.8(1) log units, respectively. The receptor is in the pro-

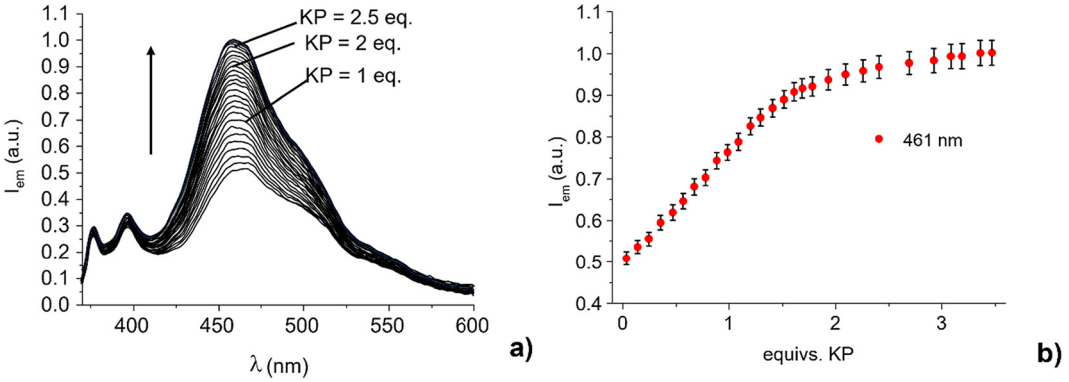

Fig. 2 (a) Fluorescence spectra of L1 and (b) plot of the emission intensity at 396 nm and 461 nm in the presence of increasing amount of KP (H_2O : EtOH 1 : 1 v/v, pH = 7, Tris 0.005 M, [L1] = 5×10^{-7} M, λ_{exc} = 360 nm). Error bars represent the standard deviation for triplicate measurements.

tonated (positively charged) form at neutral pH (the main form present in solution at neutral pH is the monoprotonated one). Therefore, it can interact *via* non-directional charge–charge interactions with the anionic carboxylate groups of ketoprofen. At the same time, the ammonium and amine groups can act as hydrogen bonding donors toward the carboxylate moiety. Finally, the pyrene units can give hydrophobic interactions with the aromatic portion of KP. The presence of multiple interaction modes, which likely act cooperatively in anion binding, may allow the formation of adducts containing more than one anionic host. This result is in good agreement with that previously found for the adduct of KP with the corresponding bis-anthracenyl derivatives of both diethylene- and triethylenetriamine, for which the formation of adducts with both 1 : 1 and 1 : 2 stoichiometry was observed.[36] Under these experimental conditions, a detection limit (LOD) of 17 μM (4.3 mg L^{-1}) was estimated for KP sensing by L1 (Fig. S9†). As reported above, L1 is in its monoprotonated form at neutral pH value, the acidic proton being localized on the central amine group. Hydrogen bonding and electrostatic interactions may occur between the carboxylate group of KP (the pK_a value of KP is 5.31 in 1 : 1 (v/v) H_2O/EtOH mixture) and the protonated central $-NH_2^+$ group of L1, as shown in Scheme 2. However, as already observed for the bis-anthracenyl derivative adducts with KP,[36] the presence of H-bonding interactions between the carbonyl function of KP and a benzyl amino-group, which contribute to the stabilization of the complex, cannot be excluded.

In polyamine compounds bearing aromatic fluorogenic units, the benzylic amine groups generally exert the most effective PET effect. Their protonation inhibits the electron transfer process due to the involvement of their lone pair in proton binding, leading to a renewal of the emission of the adjacent fluorogenic unit. This would suggest that interaction of the carboxylate group of KP induces a proton transfer process from the central amine group to a benzylic amine, with a consequently reduced PET effect and increased excimer emission.

To corroborate this suggestive hypothesis, we performed ^{1}H NMR titration by adding KP to an aqueous solution of L1.

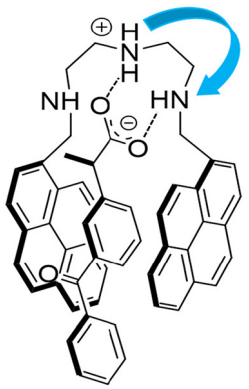

Scheme 2 Proposed interaction mode between KP^- and L1 in its monoprotonated form.

3.2.2 ^{1}H NMR titrations. ^{1}H NMR experiments were performed by adding increasing amounts of KP or L1 to a solution of L1 and KP, respectively, at fixed concentration in D_2O/DMSO-d_6 1 : 4 (v/v) mixture at neutral pH. This solvent mixture was chosen to avoid precipitation of L1 adducts with KP observed in 1 : 1 D_2O/EtOH mixture at the concentration used in ^{1}H NMR experiments (1×10^{-2} M). As shown in Fig. 3, the increase in KP concentration in an L1 solution induces a progressive downfield shift of the resonance of both the methylene bridge 1_{AL} (see Fig. 3 for atom numbering) and the methylene groups 2_{AL} adjacent to the lateral amine groups, while the chemical shift of the signal relative to the 3_{AL} methylene group remains unchanged.

In aliphatic polyamines, protonation and deprotonation processes are accompanied by a downfield and upfield shift, respectively, of the signal of the adjacent methylene units.[49] Therefore, the downfield shift of the resonance of methylene groups 1_{AL} and 2_{AL} can be ascribed to a proton transfer process from the central protonated amine group to the benzylic one upon KP binding. The increased positive charge on the nitrogen atom adjacent to the fluorophore can induce an inhibition of the PET process, justifying the partial restoration

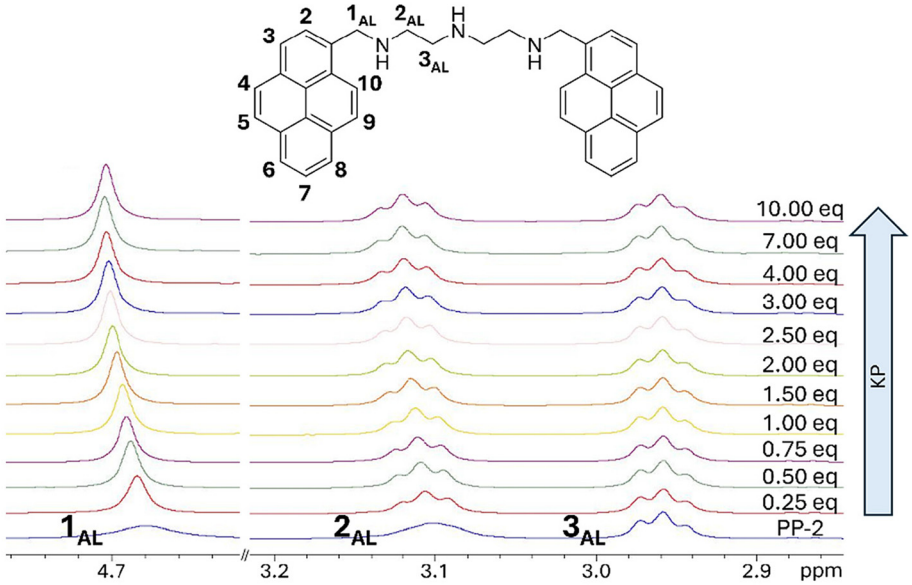

Fig. 3 Aliphatic signals of the ^{1}H NMR spectra of L1 at pH 7 in the presence of increasing amounts of KP (D_2O/DMSO-d_6 1 : 4 v/v, [L1] = 1×10^{-3} M).

of the fluorescence emission. The aromatic signals of pyrene are not affected by the interaction with the substrate, as shown in Fig. S10,† suggesting that the aromatic units of receptor and substrate are not involved in substrate coordination *via* π-stacking interactions, at least in the ground state. The proposed interaction mode in the ground state is confirmed by the analysis of the shift of the signals of KP, in which both the signals relative to the CH and CH_3 groups of KP are not significantly shifted, as displayed in Fig. S11 and S12.†

3.3 Optical properties of L1-based optodes

To transfer the optical signal of bis-pyrene-polyamine receptors in the presence of KP from solution into all-solid-state fluorimetric optical sensors, we investigated the properties of PVC plasticized membranes doped with L1·3HCl and L1 as 'free' amine, both deposited on three different solid supports (FP, CC and GS, see Experimental section for details). In total, 7 membrane compositions were prepared, as summarized in Table 1. Due to the low solubility of L1·3HCl in the solvent (THF) used for membrane Mb1.1 cocktail preparation, the optical properties of membranes Mb1.2–Mb5 doped with the non-protonated L1 (present in oil form) ligand were further studied.

TDACl and TDMACl (in membrane Mb5) anion-exchangers were added to membrane cocktails in 1 : 1, 1 : 2 or 1 : 3 ratio with respect to L1 receptor to stabilize membrane neutrality and ensure the analyte anions' membrane permselectivity. The influence of L1 protonation state in the membrane phase as well as the plasticizer nature on the optical properties of tested membranes and their sensitivity and selectivity toward ketoprofen have been also investigated.

As expected, preliminary tests on the optical response of membrane Mb1.2 deposited on CC support have shown the preferable binding of KP compared to ibuprofen (IBU) and benzoate anions, which were tested as potential interfering ions. However, an evident luminescence signal quenching was registered upon KP concentration increase, in contrast to the L1 behavior in solution (Fig. S13†). A similar response was registered for Mb1.2 spots deposited on glass and filter paper support, thus evidencing the necessity of careful tuning of the fluorophore protonation state and competitive salt-bridging effects among the fluorophore and target KP^- and/or Cl^- ions coming from the anion-exchanger or other interfering ions. To clarify these phenomena, a new series of membranes was prepared, in which 3 equivalents of protons (H^+), in the form of trifluoroacetic acid (TFA), were introduced into the freshly pre-

Table 1 Membrane compositions of optodes based on bis-pyrene polyamine receptors L1·3HCl and L1

Membrane	Ligand	Anion-exchanger	Ligand : anion exchanger, molar ratio	Plasticizer	TFA
Mb1.1	L1·3HCl		1 : 0.5	TOP	—
Mb1.2			1 : 0.7	TOP	—
Mb1.3			1 : 0.7	TOP	3 equiv.
Mb2	L1	TDACl	1 : 0.7	DOS	3 equiv.
Mb3			1 : 0.7	DOS	—
Mb4			1 : 1.5	DOS	3 equiv.
Mb5		TDMACl	1 : 2.8	DOS	3 equiv.

pared membranes (Mb1.3, Mb2, Mb4, and Mb5) to protonate the L1 ligand directly in the membrane phase.

The DOS plasticizer with lower dielectric constant (ε_{DOS} = 4.0 *vs.* ε_{TOP} = 7.9) was used instead of highly anion-solvating and basic TOP plasticizer for membranes Mb2–Mb5 preparation. To study the influence of the anion-exchanger, the ratio of L1/anion-exchanger was changed from approximately 1 : 1 to 1 : 1.5 and 1 : 3 equiv. in membranes Mb3, Mb4 and Mb5, respectively. Moreover, to keep pH at a constant value, all the measurements were done in 0.01 M Tris/HCl pH 7.00 buffer. Under these conditions, KP is completely ionized, considering that its pK_a is 4.45.

3.3.1 Ligand protonation state. In the development of fluorescent sensors, a "turn on" response is typically preferred over a "turn off" one. The use of L1·3HCl receptor for KP optical sensor development would hence be the best choice since the interaction of the L1·3HCl-protonated polyamine chain with the carboxylate group of KP (in anionic form at pH 7) induces a translocation of the acidic proton within the triamine chain, resulting in the increase of the L1·3HCl excimer emission. This "turn on" optical signal can be used to detect KP in aqueous media, as reported in section 3.2. However, L1·3HCl is not soluble inside the PVC membrane cocktails. Therefore, the non-protonated L1 receptor was selected due to its higher solubility in the membrane phase and further protonated directly inside the membrane through the addition of 3 equiv. of trifluoroacetic acid, TFA (with respect to L1 amount). Indeed, it was experimentally confirmed and illustrated in Fig. 4 that L1 protonation in the membrane resulted in an emission switch on for TFA-doped membrane Mb5 upon KP binding, while the non-protonated L1 in the presence or absence of KP maintains the system in its non-emissive state in membrane Mb3 (no TFA added, see Table 1).

Moreover, considering the acid–base properties of L1 in solution (see section 3.1), the receptor is most likely present in the membrane as a monoprotonated species, with the acidic proton localized on the central amine group of the triamine chain, making it form 1 : 1 or 1 : 2 receptor to analyte adducts.

3.3.2. Anion-exchanger influence. The presence of the protonated form of L1 receptor is necessary to obtain the membrane switch on fluorescence response toward KP. At the same time, in order to promote the flux of analyte KP ions inside the membrane phase and ensure membrane electroneutrality, the incorporation of lipophilic cationic sites in the form of TDACl anion-exchanger is required. Moreover, the anion-exchanger amount introduced inside the membrane in various ratios to the ligand may elucidate the formed complexes' stoichiometry. In the membrane phase, the formation of a 1 : 1 ligand to KP complex is prevalent and the 1 : 1 molar ratio of lipophilic TDA^+ cations with respect to the carrier L1 would be sufficient to stabilize the ion-exchange process. However, the trifluoroacetate anions from TFA will remain in the membrane phase due to their higher lipophilicity, while smaller and more mobile Cl^- anions from TDACl will be quickly leached into the solution. Hence, additional TDA^+ sites are essential for maintaining the membrane neutrality and ion-exchange efficacy. The overall equilibrium, which ensures the mass balance of neutral and charged species in the membrane, can be represented as follows.

$$\mathrm{L1_{org} + KP^-_{aq} + 3H^+_{org} + 3TFA^-_{org} + 3TDA^+_{org} + 3Cl^-_{org}} \rightleftarrows \mathrm{L1\text{-}H^+_{org}(KP^-_{org}) + 2H^+_{aq} + 3TFA^-_{org} + 3TDA^+_{org} + 3Cl^-_{aq}}$$

where $L1_{org}$, KP^-_{aq} corresponds to the neutral ligand L1 form in the membrane phase and ketoprofen anion (deprotonated form) in solution, respectively. Additionally, the asymmetric anion-exchanger, for instance, TDMACl, may better stabilize the asymmetric complex between KP and L1 in its monoprotonated form given in Scheme 2 and enhance the sensor's optical response to ketoprofen.

The tests on membranes Mb1.3–Mb5 response to KP were run in the concentration range of 2.0 μM–0.1 mM (two orders of magnitude of KP^- ions concentration) and corresponding to 1–20 equiv. ratio of L1 in the membrane and KP in the analyzed solution.

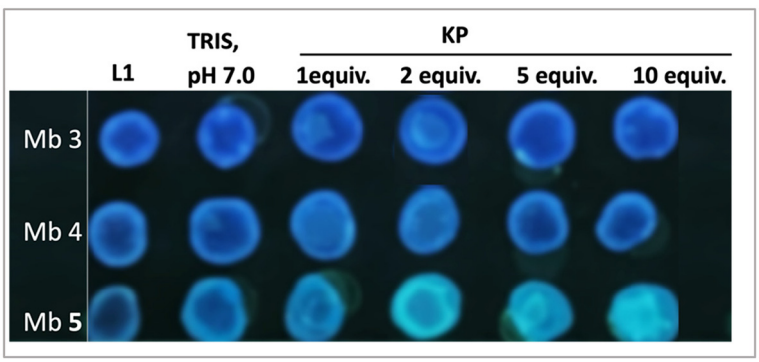

Fig. 4 Photogram of L1-based all-solid-state optodes deposited on the glass support GS to increasing concentrations of KP (1–10 equiv.) on 0.005 M Tris pH 7.0 background solution. In membrane Mb3, the L1 ligand is in its not-protonated form, and in membranes Mb4 and Mb5, 1.5 and 2.8 equiv. of TFA, respectively, were added to protonate L1 directly in the membrane phase. The image was acquired from 10 cm distance with a common smartphone, λ_{exc} = 365 nm.

The increase in the fluorescence intensity of sensing spots upon the excitation at 365 nm as a function of the growing concentration of KP was recorded, and this change was strongly correlated to the L1/anion-exchange ratio. Thus, as shown in Fig. 5, in comparison to the membranes Mb1.3–Mb3 doped with 1 equiv. of TDACl, Mb4 and especially Mb5 containing 2 and 3 equiv. of anion-exchanger, respectively, have shown the best response in a wider linear range of KP concentration. The best optical response in all the tested concentration range with R^2 = 0.984 was registered for membrane Mb5, containing 1 wt% of L1, 3 equiv. of TFA, and 3 equiv. of asymmetric TDMACl anion-exchanger.

3.3.3 Effect of plasticizer and solid support selection. The nature of the plasticizer has a smaller influence on the KP response of optodes. Thus, a similar slightly emissive response was registered at low KP concentrations (2×10^{-6}–1×10^{-5} M) for membranes Mb1.3 and Mb2 having the same composition but plasticized with TOP and DOS, respectively (Fig. 5). However, at higher KP concentrations, a more basic TOP impairs the membrane Mb1.3 response faster in the non-emissive state, in comparison to the DOS-plasticized membrane Mb2, for which the luminescence intensity decreases in a lower degree. This effect can be also due to the difference in TOP and DOS polarity (ε_{DOS} = 4.0 *vs.* ε_{TOP} = 7.9) and solvating properties, influencing the mobility and rigidity of L1 arms inside the membrane phase and vary its ability to approach KP^- ions upon the binding step to a different degree and further excimer interaction between the two pyrene groups, responsible for switch on optode response. Indeed, some small enhancement in optical response was registered for DOS-plasticized membranes in comparison to the TOP-plasticized Mb1.3; hence, only DOS-plasticized membranes' selectivity and analytical applications have been further tested.

To acquire the 2D images of all-solid-state optodes prepared by the drop-casting of a small amount (2 μL) of L1-doped PVC membranes on a solid support, a conventional smartphone was used. Two cellulose-based materials, a filter paper (FP) and color catcher tissue (CC) treated/non-treated with 0.005 M Tris pH 7 buffer solution, and glass slides (GC) were employed to test the KP response in the fluorescence readout mode. The laboratory UV-lamp operating at a wavelength of 365 nm served as an excitation light source. While no significative differences were registered for optodes on CC, a clear luminescence intensity variation for previously selected best membrane composition, Mb5, containing 1 wt% of L1, 3 equiv. of TFA, and 3 equiv. of TDMACl anion-exchanger, was observed on GS and non-treated FP. The obtained calibration curves and corresponding photos are shown in Fig. S14.† Notably, the faster optical response of PVC membranes deposited on FP in comparison to the GC support (fully luminescent at the 5th day after the exposure of KP solutions) indicates FP as the most adapted solid support material for optodes development. While the diffusion of KP solutions inside the membrane deposited on GS support is limited and could occur only from the external top side of the membrane, the faster response of FP-based optodes is due to high permeability of the FP support and possible diffusion of the sample solution inside the membrane phase not only top down but also laterally and from the bottom side. For this reason, further tests on selectivity and KP detection in pharmaceutical compositions were run for optodes on FP support. Moreover, GS and FP are eco-friendly and cost-effective materials, providing "green solutions" in the development of all-solid-state optical sensors.

3.3.4 Selectivity tests in solution and for all-solid state optodes. Efficient probes for analytes should feature selectivity in substrate sensing. Previous results suggest that electrostatic interactions between the carboxylate group of the analyte and the protonated amine group of the polyamine chain, along with H-bonding between the carbonyl group of the anion and a benzylic nitrogen atom of L1, play a key role in KP sensing by the receptor at pH 7. Even if aromatic interactions are not significantly involved (as demonstrated by ^{1}H NMR titrations, see above), an overall hydrophobic effect can contribute to improve the complex stability. These outcomes are also supported by the results of fluorimetric titrations performed by adding increasing amounts of carboxylate anions with smaller

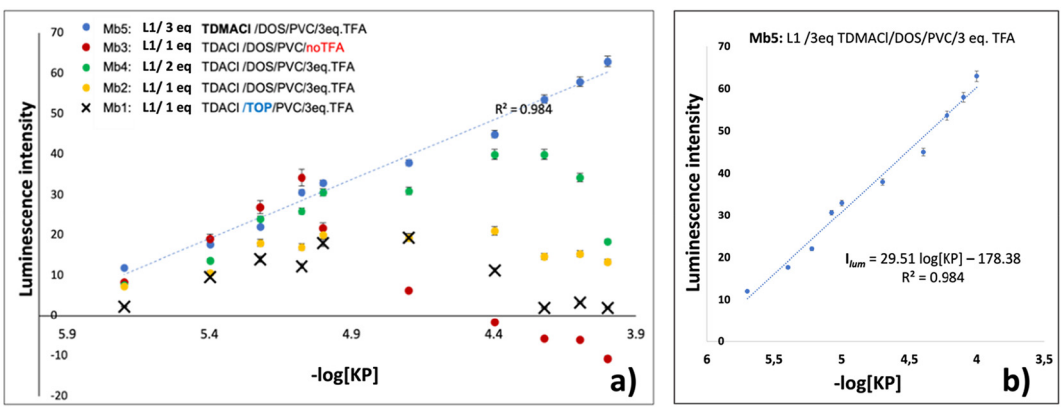

Fig. 5 (a) Luminescence intensity variation of L1-doped membranes Mb1.3–Mb5 deposited on the GS substrate upon KP concentration variation; (b) details of optical response the optimum membrane Mb5 to KP, n = 3. λ_{exc} = 365 nm.

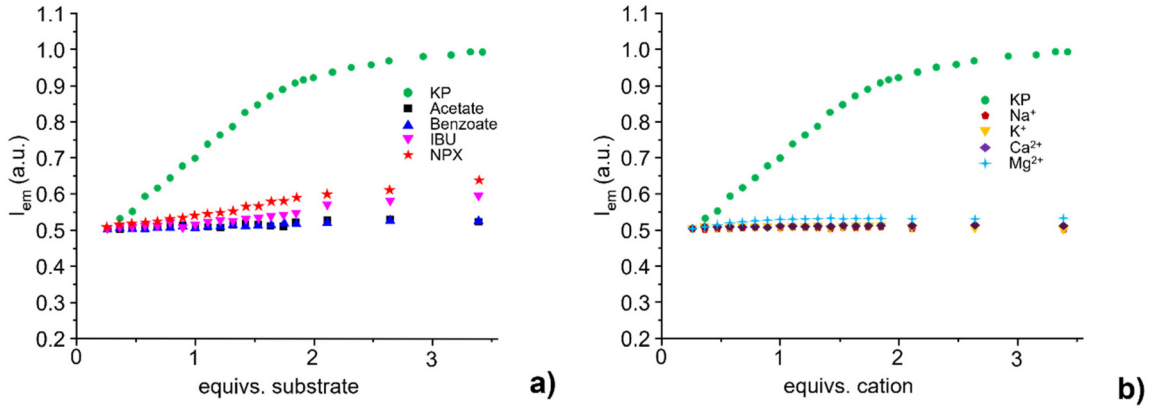

Fig. 6 Emission intensity at 495 nm of L1 in the presence of increasing amounts of (a) KP, acetate, benzoate, ibuprofen (IBU), naproxen (NPX) and (b) Na^+, K^+, Ca^{2+}, Mg^{2+}. H_2O : EtOH 1 : 1 v/v, pH = 7, Tris 0.005 M, [L1] = 5×10^{-7} M, λ_{exc} = 360 nm.

hydrophobic units, which do not feature any carbonyl functions, to a solution of L1 buffered at pH 7 (Fig. 6). Indeed, the emission intensity is only slightly affected by the addition of carboxylate anions different from KP, such as acetate, benzoate, and ibuprofen (IBU), as shown in Fig. 6a. This would indicate that weaker interactions occur between the receptor and the smaller carboxylate anions, suggesting that the overall hydrophobic character of L1 and H-bond formation contributes to the stabilization of adducts with KP, which contains a benzophenone moiety, as compared to less hydrophobic carboxylates. A somewhat higher increase was observed for the more hydrophobic naproxen (NPX) anion. However, this change in emission is remarkably less significant when compared to the enhancement observed in the presence of KP. This supports the hypothesis that H-bonding between the carbonyl group of KP and the amine group of the aliphatic chain of L1 gives an important contribution to the stabilization of the adduct, as discussed above. Moreover, the fluorescence response of L1 is not affected by the presence of some common cations in the solution found in environmental and biological matrices, such as Na^+, K^+, Ca^{2+} and Mg^{2+} (Fig. 6b), in keeping with the poor binding ability of linear polyamine ligands towards alkali and alkaline-earth metal cations in aqueous solution.[50]

The selectivity evaluation of all-solid-state optodes indicated the highest influence of KP through the analysis of luminescence intensity in the blue channel (Fig. 7 and Fig. S15†). The selectivity coefficients of all-solid-state optodes with Mb5 were calculated by a modified separate solution method (SSM) as previously reported[51] and are listed in Table 2. Details on the optodes' selectivity evaluation are provided in section S5 of ESI.† No significant influence from the parent compounds such as naproxen, ibuprofen, and benzoate, which can all be present simultaneously in pharmaceutical formulations, were observed. Likewise, the optical response of the L1-based membrane (Mb5) towards KP was not affected either by other highly lipophilic anions tested, such as perchlorate (ClO_4^-) and thiocyanate (SCN^-), which do not contain carboxyl groups (–COOH) in their structures, or by all the tested interfering cations (Table 2 and Fig. S16†), were in good accordance with selectivity tests run in the solution.

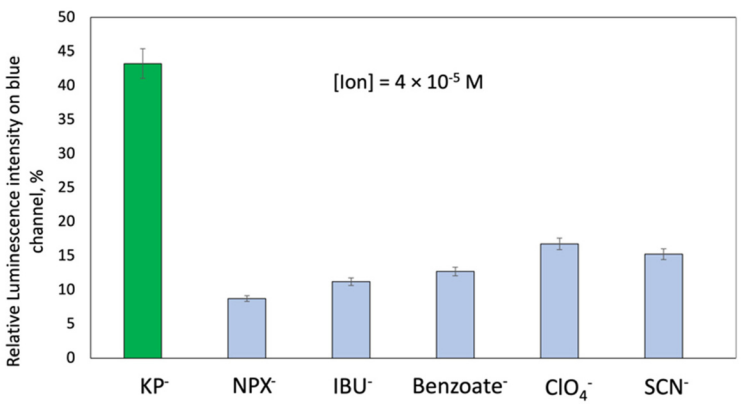

Fig. 7 Relative luminescence intensity of membrane Mb5 sensing spots on the blue channel in the presence of equal amounts of KP^-, naproxen (NPX^-), ibuprofen (IBU^-), benzoate ($Benzoate^-$), ClO_4^- and SCN^- interfering anions. [Ion] = 4×10^{-5} M, pH = 7.0, Tris 0.005 M, and λ_{exc} = 365 nm.

Table 2 Selectivity coefficients of the all-solid-state L1-based optode with Mb5, evaluated *via* a modified SSM method in solutions of various interfering ions. [Ion] = 8 × 10^{-5} M, pH = 7.0, Tris 0.005 M, λ_{exc} = 365 nm, and n = 3

Interfering ion[a]	log $K_{KP/ION}$
NPX^-	−2.21
IBU^-	−2.66
$Benzoate^-$	2.70
ClO_4^-	−2.74
SCN^-	−2.94
Na^+	−2.50
K^+	−2.22
Mg^{2+}	−4.78
Ca^{2+}	−4.98
Zn^{2+}	−5.79
Cu^{2+}	−6.31

[a] KP was considered as a primary ion; the slope of the semilogarithmic calibration curve toward KP ions was used to calculate log $K_{KP/ION}$; see ESI† for calculation details.

In Table 3, the comparison of the main characteristics of NSAIDs optical sensors previously reported in the literature[16–19,32,36,52–57] and the characteristics of the developed all-solid-state KP optode in this work based on protonated bis-pyrene polyamine receptor L1 is reported. The wide linear range of response, low detection limit, together with easy application procedure and low operational costs of the developed all-solid-state optical sensor, demonstrate its potential for KP assessment.

3.4 KP assessment in pharmaceutical compositions

The KP amount in pharmaceutical composition OkiTask by Dompé was estimated with planar all-solid-state optodes based on Mb5 membrane deposited on FP support since this membrane has shown the best analytical characteristics and wider dynamic optical response range. The application of the double addition method has shown the possibility to determine the

Table 3 Comparison of the main properties of optical chemical sensors for KP and other NSAIDs reported in the literature with the developed all-solid-state KP optode based on the protonated bis-pyrene polyamine receptor L1

Ligand	Optical output, working media	Sensing range	Limit of detection	Ref.
Polyethyleneimine passivated copper-doped CdS quantum dots and zinc oxide nanorods	Fluorescence quenching Tap water, lake water, waste water and human urine samples	0.05–35.5 μM	1.36 nM	16
CdSe/ZnS core–shell nanoparticles (chiral quantum dots) (QDs) bearing a chiral organic ligand	Fluorescence quenching; enantioselective recognition of KP	50.0×10^{-8} to 250.0×10^{-4} M	—	17
One-pot water-dispersed chitosan stabilized silver nanoparticles (AgNPs)	Fluorescence quenching Aqueous solutions pH 4.00, Ketorolac ampules, spiked river water	0.05 to 0.4 μM	—	18
Carbon Dot core Molecularly Imprinted Polymer	Fluorescence quenching Aqueous solutions, human serum and urine samples	0.039 to 3.9 μM	0.01 μM	19
MIPs with rhodamine B fluorescein-functionalized	Fluorescence quenching water/ethanol 2 : 1 (v/v) mixture	1–20 μM (NPX) 1–10 nM (KP)	0.27 μM (NPX); 0.011 μM (KP)	32
Bis-anthracene substituted polyamines	Fluorescence enhancement Water/EtOH 50 : 50 (v/v) solutions, pH 7.00	0–3 equiv. of KP	0.21 μM (L1); 0.28 μM (L2)	36
3,3′-bis[*N*,*N*-bis(pyridine-2-ylmethyl) aminomethyl]-2,2′-dihydroxybiphenyl (L) complex with Zn^{2+}, $[Zn_2(H-2L)]^{2+}$	Fluorescence quenching Water/CH_3CN 80 : 20 (v/v) solutions, pH 10.00	0–10 equiv. of KP and IBU	—	52
Carbon quantum dots in silica molecularly imprinted polymer (CQDs-SiO_2@MIP)	Fluorescence quenching, distinction between *S*- and *R*-enantiomers. Solutions on 0.05 M acetate buffer, pH = 4.00 background	0.5–35.0 μM for S-NPX; 0.5–30.0 μM for R-NPX	0.20 μM (S-NPX); 0.37 μM (R-NPX).	53
Bis-squaramide receptors	Specific fluorescence quenching of L1 and L2 to KP CH_3CN/DMSO solution 9 : 1(v/v); paper strip-test able to work in water	0–5 equiv. of KP, NPX, Benz-	—	54
Hollow core microstructure optical fibers modified with deep eutectic solvent based on natural monoterpenoid and fatty acid.	HC-MOF transmission spectra were recorded over the wavelength range of 400–800 nm Human urine samples spiked with KP, mefenamic acid, diclofenac, flurbiprofen, indomethacin	0.1–3 mg L^{-1} of NSAIDs	3 μg L^{-1} for KP	55
ITO-LMR probe ITO electrode	Lossy-mode resonance (LMR) effect for KP detection Aqueous solutions upon electropolymerisation of KP on ITO probe	0.25–250 μg mL^{-1}	0.5 mM	56
AgNPs in solution	Fluorescence quenching Pharmaceutical and prepared dosage forms, spiked human plasma	0.5–5.0 mg mL^{-1}	—	57
Protonated L1 (*N*1,*N*3-bis(1-pyrenylmethyl) diethylenetriamine) ligand inside PVC-based membrane and sensor array	Fluorescence enhancement In water/ethanol 1 : 1 (v : v) solution; on-paper and on-glass all-solid-state optode for aqueous KP solutions	2 μM–0.1 mM 0.5–20 equiv. KP	0.84 μM (0.21 mg L^{-1})	This work

Table 4 Results of KP determination in OkiTask formulation using the developed optode based on the bis-pyrene polyamine receptor L1, n = 6

[KP] real	[KP] found	RSD, %	Recovery, %
2.00×10^{-5} M	2.04×10^{-5} M	2.1	102

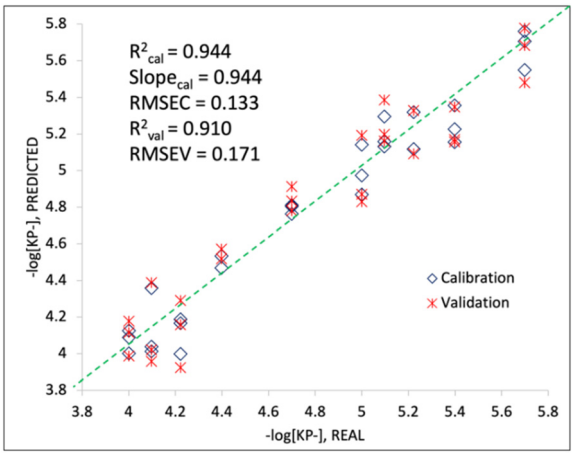

Fig. 8 PLS1 regression model based on the luminescence response of the all-solid-state planar optical sensor array in KP aqueous solutions of different concentrations.

KP amount in unknown samples with a relative error, RSD of 2.1% and recovery of 102%, as shown in Table 4, which indicates the suitability of L1 receptor for the fluorimetric detection of ketoprofen in real samples.

3.5 Multisensor approach for KP low detection limit lowering

Finally, membranes Mb1.3-Mb5 deposited on GS were used in multisensory arrangement to lower the KP detection limit. The membranes' luminescence intensities were measured simultaneously in individual aqueous solutions of KP in 2×10^{-6}–1×10^{-4} M concentration range. The obtained data matrix was used to construct the PLS1 model to correlate optical sensor array output to the KP concentration in calibration solutions (Fig. 8).

The PLS1 regression model (R^2 = 0.944, RMSEV = 0.17 log [KP], 3 PCs, 96% of total variance, 30 samples, 4 variables – luminescence intensity, RGB optical intensities) permitted to improve the KP detection limit to 0.84 μM (0.21 mg L^{-1}).

4. Conclusions

This study investigates a tri-amine receptor with two pyrene fluorogenic groups, in its protonated L1·3HCl and non-protonated L1 forms, for detecting the non-steroidal painkiller ketoprofen (KP). Results highlight that coupling a polar, hydrophilic structure with two large hydrophobic units can create a molecular receptor capable of forming stable complexes with KP. Optical studies of L1 in a 1 : 1 (v/v) water/ethanol solution at neutral pH revealed salt-bridging interactions between the carboxylate group of KP (in its anionic form at pH 7) and the protonated polyamine chain of the receptor. This interaction induces a significant enhancement of the 396 nm excimer emission band. Coordination of KP also triggered a translocation of the acidic proton within the triamine chain from the central nitrogen to the benzylic nitrogen, inhibiting the PET process from the triamine chain to the excited fluorophores.

The receptor's optical signal was used to develop an all-solid-state sensor based on L1 incorporated into PVC membranes for the optical sensing of KP in aqueous media. The sensor composition was optimized by considering the impact of different membrane components on the optical response. The best response was achieved with membrane Mb5, containing 1 wt% L1, 3 equivalents of TFA, and 3 equivalents of asymmetric TDMACl anion-exchanger. Various solid supports were tested. Paper and glass were selected due to their cost-effectiveness and environmental friendliness. Selectivity tests showed minimal interference from ions and other active pharmaceutical ingredients, including naproxen, ibuprofen, and benzoate. The developed sensor was successfully applied to analyze the OkiTask pharmaceutical formulation, with an RSD of 2.1% and a recovery of 102%. This work demonstrates that polyamine chains coupled with fluorescent hydrophobic moieties provide an effective strategy for developing optical KP chemosensors with high stability, fluorescence response, and selectivity. Additionally, the optical sensor array based on bis-pyrene-substituted receptors (Mb1.3–Mb5) offers a fast and indirect method for screening and discriminating between common non-steroidal painkillers, reducing the detection limit of KP from 4.3 mg L^{-1} to 0.21 mg L^{-1}.

Data availability

The data supporting this article have been included as part of the ESI.†

The data analysis scripts of this article are freeware and available online: Colorpicker (**https://imagecolorpicker.com/**) ImageJ (**https://ij.imjoy.io/**).

Conflicts of interest

There are no conflicts to declare.

Acknowledgements

Authors acknowledge financial support from MIUR (PRIN 2017 project 2017EKCS35). L. Lvova acknowledges financial support from Tor Vergata University (project ORIENTATE). A. Bencini, M. Innocenti and G. M. Romano thank Regione Toscana for financial support of the MetalRec Project (CUP B97G23000210009) within the program "Progetti di alta formazione attraverso l'attivazione di assegni di ricerca nell'ambito della transizione verde".

References

1 P. M. Brooks and R. O. Day, *N. Engl. Med.*, 1991, **324**, 1716–1725.
2 **https://www.nhs.uk/conditions/nsaids/**.
3 N. Halfter, E. Espinosa-Cano, G. M. Pontes-Quer, R. A. Ramírez-Jiménez, C. Heinemann, S. Möller, M. Schnabelrauch, H. P. Wiesmann, V. Hintze and M. R. Aguilar, *J. Funct. Biomater.*, 2003, **14**, 160.
4 E. Koumaki, D. Mamais and C. Noutsopoulos, *J. Hazard. Mater.*, 2017, **323**, 233–241.
5 K. Świacka, A. Michnowska, J. Maculewicz, M. Caban and K. Smolarz, *Environ. Pollut.*, 2021, **273**, 115891.
6 P. Izadi, P. Izadi, R. Salem, S. A. Papry, S. Magdouli, R. Pulicharla and S. K. Brar, *Environ. Pollut.*, 2020, **267**, 115370.
7 E. Tyumina, M. Subbotina, M. Polygalov, S Tyan and I. Ivshina, *Front. Microbiol.*, 2023, **14**, 1200108.
8 J. Wilkinson, P. S. Hooda, J. Barker, S. Barton and J. Swinden, *Environ. Pollut.*, 2017, **231**, 954–970.
9 L. M. Gomez-Olivan, *Non-Steroidal Anti-Inflammatory Drugs in Water*, Springer International Publishing, 2020.
10 Y. Fan, Y. Feng, S. Da and Z. Wang, *Talanta*, 2005, **65**, 111–117.
11 M. J. Martin, F. Pablos and A. G. Gonzalez, *Talanta*, 1999, **49**, 453–459.
12 M. El-Sadek, S. El-Adl, M. Abou-Kull and S. M. Sakr, *Talanta*, 1993, **40**, 585–588.
13 J. Lenik, *J. Anal. Chem.*, 2012, **67**, 543–549.
14 M. Y. Fares, N. S. Abdelwahab, M. A. Hegazy, M. M. Abdelrahman, A. M. Mahmoud and G. M. El-Sayed, *Anal. Sci.*, 2022, **38**, 23–37.
15 G. Picci, S. Farotto, J. Milia, C. Caltagirone, V. Lippolis, M. C. Aragoni, C. Di Natale, R. Paolesse and L. Lvova, *ACS Sens.*, 2023, **8**, 3225–3239.
16 S. Chen, S. Zhou, J. Fu, S. Tang, X. Wu, P. Zhao and Z. Zhang, *Anal. Methods*, 2021, **13**, 2836–2846.
17 T. Delgado-Pérez, L. M. Bouchet, M. de la Guardia, R. E. Galian and J. Pérez-Prieto, *Chem. – Eur. J.*, 2013, **19**, 11068–11076.
18 M. Mabrouk, S. F. Hammad, A. A. Abdella and F. R. Mansour, *Colloids Surf., A*, 2021, **614**, 126182.
19 S. Bhogal, K. Kaur, S. Maheshwari and A. K. Malik, *J. Fluoresc.*, 2019, **29**, 145–154.
20 Y. Liu, T. Minami, R. Nishiyabu, Z. Wang and P. Anzenbacher Jr., *J. Am. Chem. Soc.*, 2013, **135**, 7705–7712.
21 T. V. Shishkanova, G. Broncová, A. Skálová, V. Prokopec, M. Člupek and V. Král, *Electroanalysis*, 2019, **31**, 2024–2031.
22 J. Han, B. Wang, M. Bender, S. Kushida, K. Seehafer and U. H. F. Bunz, *ACS Appl. Mater. Interfaces*, 2017, **9**, 790–797.
23 X. Liu, N. Zhang, J. Zhou, T. Chang, C. Fang and D. Shangguan, *Analyst*, 2013, **138**, 901–906.
24 D. Zhang, S. Li, R. Lu, G. Liu and S. Pu, *Dyes Pigm.*, 2017, **146**, 305.
25 J. Li, Y. Chen, T. Chen, J. Qiang, Z. Zhang, T. Wei, W. Zhang, F. Wang and X. Chen, *Sens. Actuators, B*, 2018, **268**, 446–455.
26 A. Garau, M. C. Aragoni, M. Arca, A. Bencini, A. J. Blake, C. Caltagirone, C. Giorgi, V. Lippolis and M. A. Scorciapino, *ChemPlusChem*, 2020, **85**, 1789–1799.
27 M. C. Aragoni, M. Arca, A. Bencini, C. Caltagirone, A. Garau, F. Isaia, M. E. Light, V. Lippolis, C. Lodeiro, M. Mameli, R. Montis, M. C. Mostallino, A. Pintus and S. Puccioni, *Dalton Trans.*, 2013, **42**, 14516–14530.
28 M. Formica, G. Ambrosi, V. Fusi, L. Giorgi, M. Arca, A. Garau, A. Pintus and V. Lippolis, *New J. Chem.*, 2018, **42**, 7869–7883.
29 D. Paderni, E. Macedi, L. Lvova, G. Ambrosi, M. Formica, L. Giorgi, R. Paolesse and V. Fusi, *Chem. – Eur. J.*, 2022, **28**, e202201062.
30 A. Garau, L. Lvova, E. Macedi, G. Ambrosi, M. C. Aragoni, M. Arca, C. Caltagirone, S. J. Coles, M. Formica, V. Fusi, L. Giorgi, F. Isaia, V. Lippolis, J. B. Orton and R. Paolesse, *New J. Chem.*, 2020, **44**, 20834–20852.
31 L. Lvova, C. Di Natale and R. Paolesse, in *Electronic Tongues Fundamentals and recent advances*, ed. F. M. Shimizu, M. L. Braunger and A. Riul Jr, IOP Publishing, Bristol, UK, 2021, pp 9–1–9–51.
32 T. Wang, Q. Li, M. Wang, J. Xu, J. Li and F. Wang, *Food Chem.*, 2023, **410**, 135419.
33 Y. Liu, T. i Minami, R. Nishiyabu, Z. Wang and P. Anzenbacher Jr., *J. Am. Chem. Soc.*, 2013, **135**, 7705–7712.
34 A. Akdeniz, T. Minami, S. Watanabe, M. Yokoyam, T. Ema and P. Anzenbacher Jr., *Chem. Sci.*, 2016, **7**, 2016–2022.
35 M. Pushina, P. Koutnik, R. Nishiyabu, T. Minami, P. Savechenkov and P. Anzenbacher Jr., *Chem. – Eur. J.*, 2018, **24**, 4879–4884.
36 G. M. Romano, L. Mummolo, M. Savastano, P. Paoli, P. Rossi, L. Prodi and A. Bencini, *Chem. Commun.*, 2022, **58**, 7022–7025.
37 (*a*) N. Busschaert, C. Caltagirone, W. Van Rossom and P. A. Gale, *Chem. Rev.*, 2015, **115**, 8038–8155; (*b*) P. A. Gale, *Chem. Commun.*, 2011, **47**, 82–86; (*c*) C. Bazzicalupi, A. Bencini and V. Lippolis, *Chem. Soc. Rev.*, 2010, **39**, 3709–3728; (*d*) C. Caltagirone and P. A. Gale, *Chem. Soc. Rev.*, 2009, **38**, 520–563; (*e*) V. Amendola, M. Bonizzoni, D. Esteban-Gómez, L. Fabbrizzi, M. Licchelli, F. Sancenón and A. Taglietti, *Coord. Chem. Rev.*, 2006, **2590**, 1451–1470.
38 (*a*) E. García-España, P. Diaz, J. M. Llinares and A. Bianchi, *Coord. Chem. Rev.*, 2006, **250**, 2952–2986; (*b*) A. E. Hargrove, S. Nieto, T. Zhang, J. L. Sessler and E. V. Anslyn, *Chem. Rev.*, 2011, **111**, 6603–6782; (*c*) E. Arturoni, C. Bazzicalupi, A. Bencini, C. Caltagirone, A. Danesi, A. Garau, C. Giorgi, V. Lippolis and B. Valtancoli, *Inorg. Chem.*, 2008, **47**, 6551–6563; (*d*) P. Mateus, R. Delgado, P. Brandão and V. Félix, *J. Org. Chem.*, 2009, **74**, 8638–8646; (*e*) A. Bianchi, K. Bowman-James and E. García-España, *Supramolecular Chemistry of Anions*, Wiley-VCH, New York, 1997.
39 J. A. Sclafani, M. T. Maranto, T. M. Sisk and S. A. Van Arman, *J. Org. Chem.*, 1996, **61**, 3221–3222.

40 Y. Shiraishi, Y. Tokitoh and T. Hirai, *Org. Lett.*, 2006, **8**, 3841–3844.
41 Y. T. Simonini Steiner, G. M. Romano, L. Massai, M. Lippi, P. Paoli, P. Rossi, M. Savastano and A. Bencini, *Molecules*, 2023, **28**, 4552.
42 M. J. Adams, J. G. Highfield and G. F. Kirkbright, *Anal. Chem.*, 1977, **49**, 1850–1852.
43 (*a*) A. Ueno, I. Suzuki and T. Osa, *J. Am. Chem. Soc.*, 1990, **62**, 2461–2466; (*b*) J. Strauss and J. Daub, *Org. Lett.*, 2002, **4**, 683–686.
44 S. Reiter, M. K. Roos and R. de Vivie-Riedle, *ChemPhotoChem*, 2019, **3**, 881–888.
45 J. Hoche, H. Schmitt, A. Humeniuk, I. Fischer, R. Mitric and M. I. S. Rohr, *Phys. Chem. Chem. Phys.*, 2017, **19**, 25002–250015.
46 G. Jones and V. I. Vullev, *J. Phys. Chem. A*, 2001, **105**, 6402–6406.
47 P. Gans, A. Sabatini and A. Vacca, *Talanta*, 1996, **43**, 1739–1753.
48 (*a*) A. Bencini, A. Bianchi, E. García-España, M. Micheloni and J. A. Ramirez, *Coord. Chem. Rev.*, 1999, **188**, 97–156; (*b*) A. Bianchi, B. Escuder, E. García-España, S. V. Luis, V. Marcelino, J. F. Miravet and J. A. Ramirez, *J. Chem. Soc., Perkin Trans. 2*, 1994, 1253–1259.
49 (*a*) C. Bazzicalupi, A. Bencini, A. Bianchi, C. Giorgi, V. Fusi, B. Valtancoli, M. A. Bernardo and F. Pina, *Inorg. Chem.*, 1999, **38**, 3806–3813; (*b*) J. Seixas de Melo, M. T. Albelda, P. Daíz, E. García-España, C. Lodeiro, S. Alves, J. C. Lima, F. Pina and C. Soriano, *J. Chem. Soc., Perkin Trans.*, 2002, **2**, 991–998.
50 F. A. Cotton and G. Wilkinson, *Advanced Inorganic Chemistry*, Wiley-Interscience, 5th edn, 1988.
51 L. Lvova, G. Pomarico, F. Mandoj, F. Caroleo, C. Di Natale, K. M. Kadish and S. Nardis, *J. Porphyrins Phthalocyanines*, 2020, **24**, 964–972.
52 D. Paderni, E. Macedi, G. E. Giacomazzo, M. Formica, L. Giorgi, B. Valtancoli, P. Rossi, P. Paoli, L. Conti, V. Fusi and C. Giorgi, *Dalton Trans.*, 2024, **53**, 9495–9509.
53 Z. Dehghani, M. Akhond and G. Absalan, *Microchem. J.*, 2021, **160**, 105723.
54 G. Picci, M. C. Aragoni, M. Arca, C. Caltagirone, M. Formica, V. Fusi, L. Giorgi, F. Ingargiola, V. Lippolis, E. Macedi, L. Mancini, L. Mummolo and L. Prodi, *Org. Biomol. Chem.*, 2023, **21**, 2968.
55 P. Pidenko, C. Vakh, A. Shishov, J. Skibina, cN. Burmistrova and A. Bulatov, *Talanta*, 2021, **232**, 122305.
56 R. Bogdanowicz, P. Niedziałkowski, M. Sobaszek, D. Burnat, W. Białobrzeska, Z. Cebula, P. Sezemsky, M. Koba, V. Stranak, T. Ossowski and M. Smietana, *Sensors*, 2018, **18**, 1361.
57 N. A. Abdallah, M. E. Fathy, M. M. Tolba, A. M. El-Brashy and F. A. Ibrahim, *RSC Adv.*, 2022, **12**, 33540.